HOW COMPARABLE ARE THE EFFECTS OF INORGANIC AND ORGANIC CARBON-BASED NANOPARTICLES ON SNOW SPECTRAL RESPONSES?

Gladimir V.G. Baranoski and Petri M. Varsa

Natural Phenomena Simulation Group, School of Computer Science, University of Waterloo
200 University Ave., Waterloo, Ontario, Canada N2L 3G1

ABSTRACT

Carbon-based nanoparticles, originating from anthropogenic actives (*e.g.*, industrial production) or natural events (*e.g.*, wildfires), can be wind-transported and deposited in snow-covered regions. These light absorbing impurities (LAIs) alter the radiative exchanges between the snow covers and their surrounding environment, affecting its ecology, hydrology and climate. Due to the serious ramifications of these processes, notably in regions markedly affected by global warming conditions, it is necessary to further the current knowledge about the extent of these impurities' impact on light propagated by snow. While it has been established that those with an inorganic origin (*e.g.*, fossil fuel combustion) have stronger light absorption capabilities, those with an organic origin (*e.g.*, biomass burning) tend to be deposited in significantly larger quantities. In this paper, we examine this tradeoff and compare the effects of these two types of LAIs, respectively known as black and brown carbon, on the spectral responses of snow samples characterized by parameter values reported for natural snowpacks. To carry out this investigation, we employed an *in silico* experimental framework and used measured reflectance and transmittance datasets as baseline references for predictive simulations.

Index Terms— snow, reflectance, transmittance, black carbon impurities, brown carbon impurities.

1. INTRODUCTION

In the last decades, increasing warming conditions are posing significant risks to the environmental sustainability of a wide range of ecosystems, particularly those located in high altitude and high latitude regions [1, 2]. Variations in the morphology and composition of snow covers found in these regions are contributing to alterations in the dynamics of a myriad of processes, from snow melting and vegetation expansion to radiative exchanges associated with local and global climate changes [3, 4].

This situation is being accentuated by the contamination of snow covers by light-absorbing impurities (LAIs), notably carbon-based nanoparticles. These carbonaceous aerosols can be wind-transported far from their emission sources and reach remote regions, where they can modify the snow and light interactions associated with the aforementioned processes [5, 6, 7]. For instance, carbon-based impurities originating from deforestation activities in the Amazon basin may end up in the Andes [8, 9]. Also, while carbon-based impurities originating from wildfires in North America and Siberia may reach the Arctic [4, 10], those originating in wildfires on South America and Australia may end up in Antarctica [11, 12].

These light-absorbing carbon (LAC) nanoparticles can be classified in two main groups, namely inorganic (black) and organic (brown) [13, 14, 15]. It is worth noting that the term "black carbon" (BC) has been employed inconsistently in the related literature. Within the context of this work, it refers to carbonaceous impurities formed during the incomplete combustion of fossil fuels (*e.g.*, motor vehicle aerosols), while the term brown carbon (BrC) refers to carbonaceous impurities associated with biomass burning (*e.g.*, wood smoke aerosols). Despite their significant contributions to the ecological, hydrological and climatological transformations observed across the planet, the understanding about the specific roles of BC and BrC impurities is still far from complete, particularly with respect to the latter [7, 10].

BC impurities are known to have stronger absorption capabilities [14] and a less episodic occurrence [7]. However, the deposition of BrC impurities may be substantially larger in natural snowpacks, on the order of parts per *million* [16] instead of parts per *billion* as in the case of BC impurities [11]. This aspect raises the question whether the larger accumulation of BrC impurities may lead to alterations on the snow covers' light attenuation mechanisms similar to those elicited by the deposition of BC impurities. We note that a comprehensive understanding about these impurities is essential for their reliable detection, both *in situ* and remotely [11, 17], and the mitigation of their detrimental influence on environmental processes affecting different biomes worldwide [10, 18].

In this paper, we address this open question using a robust *in silico* approach supported by measured data obtained from natural snowpacks. More specifically, our investigation was conducted using a first-principles model for light interactions with snow, known as SPLITSnow (*SP*ectral *LI*ght *T*ransport

Thanks to NSERC (grant 108339) for funding.

in *Snow*), whose ray-optics formulation was expanded [19] to predictively simulate light attenuation effects elicited by the deposition of BC and BrC nanoparticles in snow samples under different water saturation states. Accordingly, we were able to obtain high-fidelity depictions of variations in the reflectance and transmittance profiles of snow samples contaminated by BC and BrC impurities under different conditions.

To the best of our knowledge, this is the first investigation comparing the effects of these carbon-based impurities on the spectral responses of snow samples that takes into account the distinct absorption capabilities of these impurities, their distinct concentrations in natural settings, as well as controlled alterations in the samples' nivological characteristics. To enable the reproducibility of our findings, we made SPLITSnow accessible for online use [20] and released the optical datasets employed in our simulations [21].

2. INVESTIGATION FRAMEWORK

2.1. Materials

In this work, we considered representative virtual samples with characteristics based on those of a real sample from a snowpack formed at the US Army Cold Regions Research and Engineering Laboratory in Hanover, USA [22]. This reference sample was selected for the following reasons. While most measurement campaigns focus on snow reflectance measurements, transmittance measurements are still scarcely reported in the literature [23]. For this sample, both reflectance and transmittance measurements were made available [22]. We were then able to employ them to assess the fidelity of our baseline simulations as described in the next section. Also, the snowpack was formed in a rural location susceptible to a relatively small amount of carbon-based contamination. This relatively low, albeit radiometrically significant, level of contamination, enabled a reliable analysis of the samples' light transmission profiles. This task would have been prone to uncertainties if one would consider high levels of contamination, which would prompt stronger light attenuation within the samples and markedly decrease their transmittances.

The default parameter values employed in the characterization of the virtual snow samples are provided in Table 1. For conciseness, more detailed information about the selection of these values based on the reference sample's nivological description is provided elsewhere [19].

We considered two groups of virtual samples. Their distinctive characteristics were the type and the concentration of their impurities. More specifically, for the samples containing BC nanoparticles, we set their concentration to 5 ng/g according to values reported for natural snowpacks in the literature [4, 24]. Similarly, for the samples containing BrC nanoparticles, we set their concentration to 500 ng/g, also considering values reported for natural snowpacks [16].

It has been recognized that different methodologies can

Table 1. Default parameter values employed in the characterization of the virtual snow samples.

Parameter	Value
Grain size range (μm)	500–1000
Grain facetness range	0.1-0.3
Grain facetness mean	0.2
Grain facetness standard deviation	0.1
Grain sphericity range	0.7–0.95
Grain sphericity mean	0.85
Grain sphericity standard deviation	0.1
Temperature ($^{\circ}C$)	-1
Water saturation	0.18
Thickness (cm)	11
Density (kg/m^3)	300

be employed to obtain appropriate values for the parameters used to quantify the absorptive properties of carbon-based impurities, namely, the reference wavelength, the mass absorption efficiency and the Angstrom exponent [19]. In this work, the selection of values for these parameters was based on the aethalometer method [15]. This choice was based on the widespread use of this method and the fact that it does not depend on auxiliary data sources [15, 25].

For consistency with related works [13, 14, 26], we elected to set the mass absorption efficiency and the reference wavelength for the BC and BrC samples to 16.619 m^2g^{-1} and 880 nm, respectively. We note that their product is equal to 14625 [19], a constant commonly employed by those works. Although other values could be chosen (*e.g.*, 31.1 m^2g^{-1} and 470 nm [26]), their product is nearly the same as that of the previous values. As for the Angstrom exponent, we selected 1 and 2 for the BC and BrC samples, respectively [13, 15]. This translates, as expected [14, 27], to the latter having relatively stronger absorption capabilities in the shorter wavelengths than in the longer wavelengths, albeit with the former remaining the dominant absorber [13].

We also note that carbon-based impurities can be found in the ice grains (through a sedimentation process) and/or in the samples' pore space (through a suspension process) [28]. In our simulations, we considered both sedimentation and suspension fractions (varying from 0 to 1 [19]) equal to 0.5.

2.2. *In Silico* Experimental Setup

Our controlled experiments consisted in the computation of directional hemispherical reflectance and transmittance curves for the selected snow samples using the SPLITSnow model [19, 29]. These curves were computed considering a spectral resolution of 5 nm, with 10^6 incident rays per sampled wavelength (λ). This number of rays was selected to ensure asymptotically convergent reflectance and transmittance values. We also considered and angle of incidence of 0° for consistency with the measurement setup employed to obtain the reference measured datasets [22].

In order to obtain a baseline for our simulations, we computed reflectance and transmittance curves for a BC sample using the default parameter values provided in Table 1, and compared them with the respective measured curves provided by Perovich [22] for the reference sample. The close agreement between the modeled and measured datasets (Fig. 1), as well as the low root mean square errors calculated for them, 0.0092 (or 0.92%) and 0.0021 (or 0.21%) for the reflectance and transmittance curves, respectively, reinforced the plausibility of the default values selected for the nivological parameters listed in Table 1.

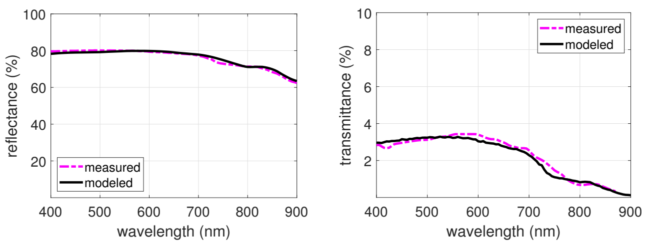

(a) Reflectance curves. (b) Transmittance curves.

Fig. 1. Modeled and measured radiometric data obtained for a selected BC sample.

We then proceeded to assess the BC and BrC samples' spectral responses with respect to six test cases (Table 2). For case W1, we used the default parameter values listed in Table 1. For the lower grain size range cases (W2 and D2) and lower density cases (W3 and D3), we set these parameters to 150-500 μm and 150 kg/m^3, respectively. For the dry state cases (D1, D2 and D3), we set the water saturation to 0.

Table 2. Test cases considered in this investigation.

Case	Description
W1	Samples in a wet state.
W2	Samples in a wet state & with a lower grain size range.
W3	Samples in a wet state & with a lower density.
D1	Samples in a dry state.
D2	Samples in a dry state & with a lower grain size range.
D3	Samples in a dry state & with a lower density.

Lastly, in order to quantify the differences between the reflectance curves obtained for each test case, we computed the mean relative differences between the corresponding curves obtained for the samples. This metric (expressed in terms of percentage) is calculated using the following formula:

$$MRD_{\rho} = \frac{1}{N} \sum_{i=1}^{N} \frac{|\rho_{BrC}(\lambda_i) - \rho_{BC}(\lambda_i)|}{\rho_{BC}(\lambda_i)} \times 100, \quad (1)$$

where $\rho_{BrC}(\lambda_i)$ and $\rho_{BC}(\lambda_i)$ represent the reflectance values obtained for the samples BrC and BC with respect to each test case, and N corresponds to the total number of wavelengths sampled with a 5 nm resolution within the spectral region of interest (400-900 nm). Similarly, to quantify the differences between the transmittance curves, we computed MRD_{τ} using Eq. 1 with the reflectance values replaced by the transmittance values obtained for each test case.

3. RESULTS AND DISCUSSION

The reflectance curves (Fig. 2) obtained for the BC and BrC samples depicted small relative differences with respect to all test cases. This is corroborated by the corresponding low MRD_{ρ} values presented in Table 3. Also, these differences were slightly more pronounced for shorter wavelengths. Although, the reduction of the samples' grain size range led to small reflectance increases (Figs. 2(b) and (e)), which is consistent with empirical data [30], the differences remained similar. They became nearly negligible, however, when we reduced the samples' density (Figs. 2(d) and (f)). Furthermore, the samples' distinct water saturation states did not affect these qualitative observations, albeit the reflectances were lower for the wet cases as expected [22].

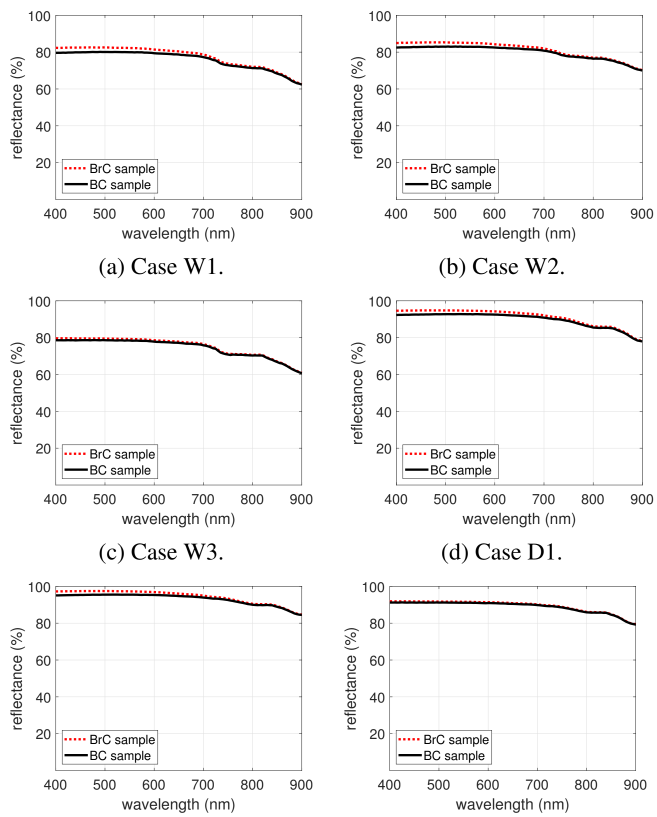

(a) Case W1. (b) Case W2.

(c) Case W3. (d) Case D1.

(e) Case D2. (f) Case D3.

Fig. 2. Modeled reflectance curves obtained for the BC and BrC samples considering the default parameters listed in Table 1 and the test cases indicated in Table 2.

The transmittance curves (Fig. 3) obtained for the BC and BrC samples, albeit having a significantly lower magnitude in comparison with the reflectance curves, depicted proportionally larger relative differences with respect to all test cases.

This aspect can also be verified by comparing the MRD_ρ and MRD_τ values presented in Table 3. Again, these differences were markedly more pronounced for shorter wavelengths, which is consistent with the wavelength-dependence of the BC and BrC impurities' absorption spectra [14, 19]. Moreover, as expected [23], the grain size range reduction led to a decrease in the transmittances (Fig. 3(b) and (e)), while the density reduction led to their increase (Fig. 3(c) and (f)), with the smaller transmittance difference being observed for cases W3 and D3. Overall, as also expected [23], the wet cases depicted larger transmittances, notably in the visible domain, than their dry counterparts.

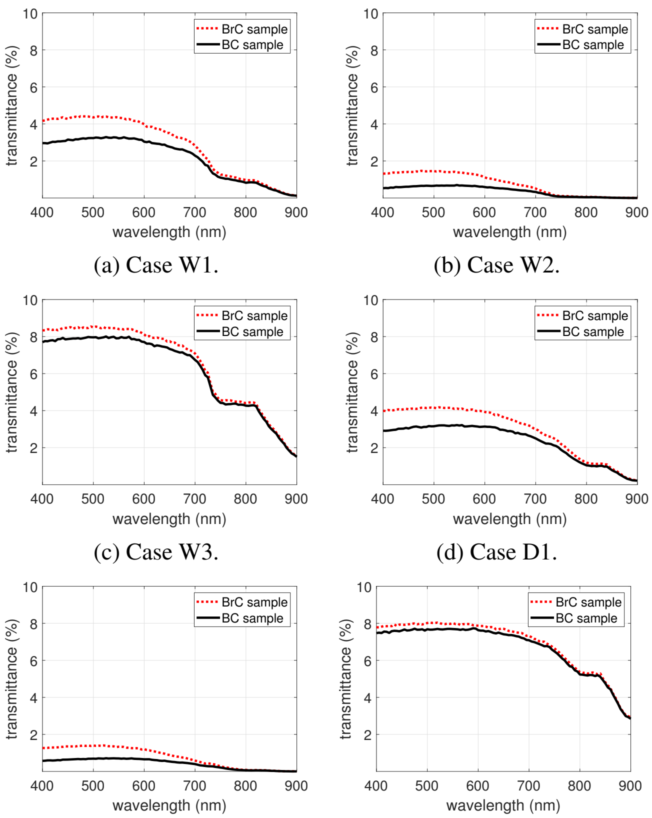

(a) Case W1. (b) Case W2. (c) Case W3. (d) Case D1. (e) Case D2. (f) Case D3.

Fig. 3. Modeled transmittance curves obtained for the BC and BrC samples considering the default parameters listed in Table 1 and the test cases indicated in Table 2.

Our preliminary findings suggest that, despite the overall weaker absorption capabilities of the BrC impurities, their occurrence in much larger amounts [16, 12] can make their impact on snow reflectance comparable to that of the BC impurities. Variations on snow nivological characteristics led to small mean relative differences, from 0.45% to 2.04% (Table 3), in the reflectances of the BrC and BC samples. On the other hand, the impact of BrC and BC impurities on snow transmittance can differ more significantly even considering the larger deposited amounts of the former. Furthermore, the corresponding mean relative differences are more susceptible to variations in the snow nivological characteristics. In our *in silico* experiments, these differences ranged from 3.11% to 76.34% (Table 3).

Table 3. MRD_ρ and MRD_τ values calculated for each test case (Table 2).

	Test Cases					
Metric	W1	W2	W3	D1	D2	D3
$MRD_\rho(\%)$	2.04	1.73	0.85	1.55	1.33	0.45
$MRD_\tau(\%)$	25.44	76.34	5.14	22.61	66.11	3.11

These observations indicate that, despite their more episodic occurrence, the contributions of BrC impurities to snow and environment interactions should not be overlooked. Thus, efforts to expand the relatively limited understanding about these contributions [7, 10] should be similar to those that have been directed to BC contributions to date. This aspect is highlighted by the fact that, while there are tangible perspectives for the reduction of BC impurities in some regions [18], the deposition of BrC impurities continues to raise in highly-sensitive regions, notably due to the increasing frequency of their originating emission events [8, 12]. The effective tackling of this timely topic will likely require the pairing of *in situ* and *in silico* experiments with remote sensing technologies based on airborne and satellite systems.

4. CONCLUSION

The deposition of carbon-based impurities in snow can alter its mechanisms of light propagation, leading to the intensification of several pivotal processes affecting different regions and their human and animal populations. Studies in this area have been primarily directed to BC nanoparticles, which are characterized by stronger light absorbing capabilities. However, the increase in the emissions of BrC nanoparticles, either from anthropogenic activities or natural events accentuated by climate changes, is gradually changing this scenario. With larger quantities of these nanoparticles being accumulated in snow covers, their role in those processes are likely to become increasingly more prominent.

In this work, we compared the overall effects of BC and BrC nanoparticles on snow spectral responses. Our preliminary findings suggest that, as their depositions tend to follow distinct trends, with policies being implemented to reduce BC emissions, their impact on snow reflectance and transmittance may reach similar levels.

To further investigate this topic, future studies should expand on the analysis of factors affecting the spectral responses of contaminated snow. These initiatives may involve simulations considering different concentrations of BC and BrC impurities, as well as distinct choices for their absorption parameters. These simulations, in turn, should complement, and be supported by, broader measurement efforts in this area.

5. REFERENCES

[1] P. Niittynen, R.K. Heikkinen, and M. Luoto, "Snow cover is a neglected driver of Arctic biodiversity loss," *Nat. Clim. Change*, vol. 8, pp. 997–1003, 2018.

[2] S.B. Rumpft, M. Gravery, O. Brönnimann, M. Luoto, C. Cianfrani, G. Mariethoz, and A. Guisan, "From white to green: Snow cover loss and increased vegetation productivity in the European Alps," *Science*, vol. 376, pp. 1119–1122, 2022.

[3] J. Zheng, G. Jia, and X. Xu, "Earlier snowmelt predominates advanced spring vegetation greenup," *Agr. Forest Meteorol.*, vol. 315, pp. 1245:1–19, 2022.

[4] Z. Zhang, L. Zhou, and M. Zhang, "A progress review of black carbon deposition in Arctic snow and ice and its impact on climate change," *Adv. Polar Sci.*, vol. 35, no. 2, pp. 178–191, 2024.

[5] J.L. Thomas *et al.*, "Quantifying black carbon deposition over the Greenland ice sheet from forest fires in Canada," *Geophys. Res. Lett.*, vol. 44, pp. 7965–7974, 2017.

[6] P.M. Rowe *et al.*, "Black carbon and other-absorbing impurities in snow in Chilean Andes," *Scientific Reports*, vol. 9, pp. 4008:1–16, 2019.

[7] M. Réveillet *et al.*, "Black carbon and dust alter the response of mountain snow cover under climate change," *Nat. Comun.*, vol. 13, pp. 5279:1–12, 2022.

[8] E.X. Bonilla *et al.*, "Contribution of biomass burning to black carbon deposition on Andean glaciers: Consequences for radiative forcing," *Environ. Res. Lett.*, vol. 18, pp. 024031:1–10, 2023.

[9] N. de Magalhães Neto, H. Evangelista, T. Condom, A. Rabatel, and P. Ginot, "Amazonia biomass burning enhances tropical Andean glaciers melting," *Scientific Reports*, vol. 9, pp. 16914:1–12, 2019.

[10] L. Yu, G. Leng, and A. Python, "Attribution of the spatial heterogeneity of Arctic surface albedo feedback to the dynamics of vegetation, snow and soil properties and their interactions," *Environ. Res. Lett.*, vol. 17, pp. 014036:1–13, 2022.

[11] R.R. Cordero *et al.*, "Black carbon footprint of human presence in Antartica," *Nature Com.*, vol. 13, no. 984, pp. 1–11, 2022.

[12] G.S. Chelluboyina, T.S. Kapoor, and R.K. Chakrabarty, "Dark brown carbon wildfires: A potent snow radiative forcing agent?," *Clim. Atmos. Science*, vol. 7, no. 200, pp. 1–10, 2024.

[13] T.W. Kirchstetter, T. Novakov, and P.V. Hobbs, "Evidence that the spectral dependence of light absorption by aerosols is affected by organic carbon," *J. Geophys. Res.*, vol. 109, no. D21208, pp. 1–12, 2004.

[14] M.R. Olson, M.V. Garcia, M.A. Robinson, P.V. Rooy, M.A. Dietenberger, M. Bergin, and J.J. Schauer, "Investigation of black and brown carbon multiple-wavelength-dependent light absorption from biomass and fossil fuel combustion source emissions," *J. Geophys. Res. Atmos.*, vol. 120, pp. 6682–6697, 2015.

[15] N.L. Briggs and C.M. Long, "Critical review of black carbon and elemental carbon source apportionment in Europe and the United States," *Atmos. Environ.*, vol. 144, pp. 409–427, 2016.

[16] N.D. Beres, D. Sengupta, V. Samburova, A.Y. Khlystov, and H. Moosmüller, "Deposition of brown carbon onto snow: Changes in snow optical and radiative properties," *Atmos. Chem. Phys.*, vol. 20, pp. 6095–6114, 2020.

[17] R. Sánchez-López, C. Mattar, C. Bravo, C. Durán-Alarcón, and T.M. Jenk, "Monitoring of light absorbing impurities (LAIs) in snow and glaciers along central Andes," *Rec. Adv. Remote Sens.*, vol. 4, pp. 1–8, 2025.

[18] D. Hao, G. Bisht, H. Wang, D. Xu, H. Huang, Y. Qian, and L.R. Leung, "A cleaner snow future mitigates Northern hemisphere snowpack loss from warming," *Nat. Commun.*, vol. 14, pp. 6074:1–10, 2023.

[19] G.V.G. Baranoski, P.M. Varsa, and H. Guan, "Black carbon impact on snow and vegetation interactions affecting environmental feedback loops and climate change," in *Proc. of SPIE, Vol. 13666, Remote Sensing for Agriculture, Ecosystems, and Hydrol. XXVII*, C.M.U. Neale, A. Maltese, C.R. Bostater, and A. Castagna, Eds., Madrid, Spain, 2025, pp. 13660W:1–19.

[20] Natural Phenomena Simulation Group (NPSG), *Run SPLITSnow Online*, School of Computer Science, University of Waterloo, Ontario, Canada, 2021, Link to model interface: http://www.npsg.uwaterloo.ca/models/splitsnow-i.php.

[21] Natural Phenomena Simulation Group (NPSG), *Snow Data*, School of Computer Science, University of Waterloo, Ontario, Canada, 2020, http://www.npsg.uwaterloo.ca/data/snow.php.

[22] D.K. Perovich, "Light reflection and transmission by a temperate snow cover," *J. Glaciol.*, vol. 53, no. 181, pp. 201–210, 2007.

[23] G.V.G. Baranoski and P.M. Varsa, "Environmentally induced snow transmittance variations in the photosynthetic spectral domain: Photobiological implications for subnivean vegetation under climate warming conditions," *Remote Sens.*, vol. 16, no. 927, pp. 1–23, 2024.

[24] S.G. Warren, "Can black carbon in snow be detected by remote sensing?," *J. Geoph. Res. Atmos.*, vol. 118, pp. 779–786, 2013.

[25] E. Weingartner, H. Saathoff, M. Schnaiter, N. Streit, B. Bitnar, and U. Baltensperger, "Absorption of light by soot particles: Determination of absorption coefficient by means of aethalometers," *J. Aerosol Sci.*, vol. 34, pp. 1445–1463, 2003.

[26] C.D. Jain, H.S. Gadahavi, T.T. Wankhede, K. Kallelapu, S. Sudhesh, L.N. Das, R.U. Pai, and A. Jayaraman, "Spectral properties of black carbon produced during biomass burning," *Aerosol and Air Qual. Res.*, vol. 18, pp. 671–679, 2018.

[27] G.W. Fuller, A.H. Tremper, T.D. Baker, K.E. Yttri, and D. Butterfield, "Contribution of wood burning to pm_{10} in London," *Atmos. Environ.*, vol. 87, pp. 87–94, 2014.

[28] L. Kou, *Black carbon: Atmospheric measurements and radiative effect*, Ph.D. thesis, Dalhousie University, Halifax, Nova Scotia, Canada, October 1996.

[29] P.M. Varsa, G.V.G. Baranoski, and B.W. Kimmel, "SPLITSnow: A spectral light transport model for snow," *Remote Sens. Environ.*, vol. 255, pp. 112272:1–20, 2021.

[30] T. Nakamura, O. Abe, T. Hasegawa, R. Tamura, and T. Ohta, "Spectral reflectance of snow with a known grain-size distribution in successive metamorphism," *Cold Reg. Sci. Technol.*, vol. 32, pp. 13–26, 2001.